FIFTH AUSTRALASIAN CONFERENCE

on

HYDRAULICS AND FLUID MECHANICS

at

University of Canterbury, Christchurch, New Zealand

1974 December 9 to December 13

STRUCTURAL CHANGES IN TURBULENT CONDUIT FLOWS BY POLYMER ADDITIVES

by

F. DURST and R.J. KELLER

SUMMARY

To date, a large number of measurements have been carried out to quantify the drastic reduction in friction losses by polymer injection into pipe and channel flows and to establish its dependence on polymer properties, polymer concentration, and flow parameters. An important observation from this previous work has been the conclusive demonstration that drag reduction is a wall phenomenon.

In the present paper experimental and theoretical investigations are described which complement rather than repeat previous research efforts. A deterministic picture of the turbulence production cycle in the wall region of a water flow is presented and a conceptional model of the structural changes resulting from the presence of polymer additives is put forward.

This physical model is corroborated by experimental investigations carried out on the flow in a vertical two-dimensional conduit (aspect ratio 10) at Reynolds numbers of approximately 10^5. Probability density distributions of the instantaneous local velocities in the flow were measured with a laser-Doppler anemometer. These measurements demonstrate that the influence of the polymer molecules is to suppress the interaction between the near wall and the log-law region leading to a reduction in turbulent drag.

F. Durst, SFB 80, University of Karlsruhe, Germany
R.J. Keller, MOW Hydraulics Laboratory, Lower Hutt, New Zealand (formerly SFB 80, University of Karlsruhe, Germany)

1. INTRODUCTION

The addition of relatively small amounts (1-10 ppm by weight are sufficient) of certain long chain polymers to a turbulent flow can result in considerably lower friction factors relative to the friction factor of the basic solvent and in the literature reductions of up to 80% have been reported. This phenomenon was first reported by Toms in 1948 (1) and has received considerable attention over the last 15 years. On the basis of many experimental studies, mainly of pipe and channel flows, several attempts have been made to correlate polymer properties and the data on friction factors. In spite of these attempts, which are summarized by Lumley (2), (3), practical applications of the phenomenon have been hampered by the lack of physical understanding of the drag reducing influence of polymers.

Experimental evidence that drag reduction is a wall phenomenon was first provided by Wells and Spangler (4), and only recently have several research workers started to relate drag reduction to structural changes in turbulent flow. It is not surprising then that an understanding of the phenomenon has only started to develop in the recent past in step with physical studies of the structure of the near wall region of turbulent wall flows.

Investigations of the structure of turbulent flows were first carried out by Kline et al. (5) using hydrogen bubbles to visualize the flow. Later work by Corino and Brodkey (6) yielded a deterministic picture of the flow in the near wall region. The qualitative picture provided by the above authors has recently been quantified by Wallace et al. (7). A summary of this work is presented in the following paragraphs.

Figure 1 shows a sketch of an individual flow motion or "event" which occurs in the near wall region and results in longitudinal and transverse velocity fluctuations. These events may be classified according to the sign of the associated longitudinal and transverse velocity fluctuations. Following the classifications of Wallace et al. (7) and Kim et al. (8), an event is a "burst" if it has a deficiency of longitudinal velocity (negative u) and moves away from the wall (positive v). An event is a "sweep" if it possesses an excess of longitudinal velocity (positive u) and moves towards the wall (negative v). The other events are referred to as "wallward interactions" (u and v both negative) and "outward interactions" (u and v both positive).

The mean Reynolds stress, $-\rho\overline{uv}$, at a point in the flow is made up of the above described individual fluid motions and Wallace et al. (7) showed that bursts and sweeps each contribute about 70% of the net stress $-\rho\overline{uv}$. They showed further that the wallward interactions and outward interactions each provide negative contributions of about 20%, making up the necessary 100% balance.

The pressure loss in turbulent flows is associated with the production and transport of turbulent energy and in turbulent wall flows production has a maximum in the near wall region. If the pressure loss decreases due to the presence of minute amounts of polymer additives in the solvent, it is justified to conclude that drag reduction is associated with a modification of the turbulent energy production near the wall. Since in a fully developed turbulent flow the entire turbulent production, distribution and dissipation cycle is in statistical equilibrium, the modification of turbulent energy production will result in an adjustment of the energy transport terms in the turbulent energy equation.

$$\underbrace{U_i \frac{\partial k}{\partial x_i}}_{\text{convection}} = \underbrace{\frac{\partial}{\partial x_i}\left[\overline{u_i\left(\frac{u_j u_j}{2} + \frac{p}{\rho}\right)}\right]}_{\text{diffusion}} \underbrace{- \overline{u_i u_j}\frac{\partial U_i}{\partial x_j}}_{\text{production}} \underbrace{+ \nu \frac{\partial^2 k}{\partial x_i \partial x_i}}_{\text{visc. diffusion}} \underbrace{- \nu \overline{\frac{\partial u_l}{\partial x_i}\frac{\partial u_l}{\partial x_i}}}_{\text{visc. dissipation}}$$

In order to explain the influence of the polymer on the production of turbulent energy in the near wall region, it is necessary to understand and explain its action on the single flow events described above. In section 2, physical explanations are given which explain the decrease in turbulence production in flows with polymer additives in terms of decreased interactions of bursts from the sublayer with the "logarithmic" flow region. Experimental evidence of this postulated influence is presented in section 3, where also mean velocity and turbulence intensity data are provided as a basis for flow predictions. All the experiments were carried out in a rectangular channel with polymer injection at one wall as a basis for future studies of interactions between boundary layers with and without polymer additives. The experimental results are discussed in section 4 and final conclusions are presented in section 5.

2. INFLUENCE OF POLYMER ADDITIVES ON DISCRETE FLOW EVENTS

In section 1 it has been pointed out that time averaged quantities such as the turbulent shear stress $-\rho\overline{uv}$ contain contributions from single, well defined flow events, referred to as bursts, sweeps, outward and inward interactions. A deeper understanding of the influence of polymer additives on these events follows from a closer examination of their formation and interaction.

One cause of bursting has been shown by Kline et al. (5) to be the result of spanwise velocity variations resulting from large scale longitudinal vorticity. Low velocity longitudinal streaks form at the wall as the result of the compression of spanwise vortices between contra-rotating longitudinal vortices. These streaks lift away from the wall, probably as the result of a strong updraft between the longitudinal vortices. Bursts formed by this mechanism, illustrated in Fig. 1, are referred to in the following as initial bursts.

Offen and Kline (9) showed by flow visualization that sweeps result from the interaction of bursts with the flow in the law-of-the-wall region. They observed further that the arrival of a sweep at the wall frequently preceded the formation of another burst . In the authors' opinion, such bursts, referred to below as secondary bursts, result from interactions of the rotational movement of the spanwise sweep motion with the flow in the near wall region. The superposition of the rotational sweep motion on the main flow creates an inflexional instantaneous velocity profile as has been observed by Kim et al. (8) and as sketched in Fig. 2. The point of inflexion moves towards the wall together with the sweep motion. The secondary bursts stem from the eventual presence of the resulting instantaneous velocity defect near the wall.

In the authors' opinion the main influence of polymer additives takes place through the prevention of the interaction of flow from the low velocity region near the wall with the flow in the region where the log-law velocity distribution holds. This means that the sweep rate and, hence, also the rate of the secondary bursting is reduced. This explanation agrees with experimental findings of Donahue et al. (10) who in a flow visualization study showed that the spatially averaged bursting rate in a drag reducing flow is lower than that for a water flow at the same wall shear stress.

The present model allows interpretations of other observed drag reduction properties. For example, the model predicts a maximum drag reduction asymptote for all turbulent wall boundary layers. This phenomenon, already extensively verified for internal turbulent boundary layer flows, may be explained as follows.

Kline et al. (5) have shown the existence of a power law correlation between bursting rate and shear velocity. Hence, the above model, which predicts a reduced bursting rate for polymer flows, also predicts drag reduction. However, since the model predicts a reduction only in the secondary bursting, maximum drag reduction occurs when this type of bursting is completely eliminated. The initial bursting, which is not affected by polymer additives, is always present.

Extensions of the model to explain the onset of drag reduction and to predict its dependence on the wall shear stress are presently being developed.

3. EXPERIMENTAL INVESTIGATIONS

3.1 Test Rig: The experiments were carried out on flows in a vertical, rectangular, perspex conduit of dimensions 30 x 3 cm which is shown schematically in Figure 3. Water was supplied to the test section via a constant head tank and a steel inlet region which provided fully developed turbulent flow at the beginning of the perspex section. The length of the steel inlet region was 4.0 m, and a smooth connection to the perspex conduit eliminated flow disturbances.

An injection system was provided on one wall at the head of the perspex test section. Polymer was injected through a shielded slot 0.5 mm wide, the details of which are given in Figure 3.

The test polymer solutions required careful preparation because the long chain molecules are subject to mechanical degradation through too vigorous stirring. A master solution of concentration 1000 ppm was carefully prepared by gentle mixing with a magnetic stirrer. The solution was then diluted to the test strength by gentle mixing with water. Finally, the test solutions were left to stand for at least 12 hours before testing to ensure full homogeneity. In the present tests the polymer Polyox Coagulant was used.

An orifice meter on the water supply line measured the water discharge. The polymer discharge was calculated from the rate of settling of the surface in the polymer tank. Pressure drop measurements, required for the calculation of wall shear stresses, were made with a manometer bank. Before any testing, the orifice meter and manometer bank were flushed with water to remove all air.

The correct functioning of the test rig was verified by measurements of pressure drop data in water flows at several Reynolds numbers. These data are plotted on a friction factor diagram in Figure 4 and show excellent agreement with the reference line for smooth conduits.

For the tests reported in this paper the polymer concentration was 100 ppm and the polymer discharge approximately equal to the discharge within the viscous sublayer ($0 \leq y+ \leq 12$). This follows the work of Wu and Tulin (11) who found that such a discharge gave appreciable drag reduction.

3.2 Measuring Technique: To obtain information on the influence of polymer additives on the structure of turbulent wall boundary layers, local instantaneous velocity measurements were carried out at different points inside the rectangular duct. The measurements were performed with a laser-Doppler anemometer as indicated schematically in Figure 3. The optical system of the anemometer consisted of an integrated optical unit which was operated in the fringe mode and was positioned on one side of the channel. The light scattered in the forward direction from small particles, which are naturally present in the water, was collected by a lens which also imaged the measuring control volume onto the mask in front of the photomultiplier. The optical system was set up following design considerations provided by Durst and Whitelaw (12) to yield approximately 100 fringes inside the measuring control volume, see Figure 5.

The signal from the photomultiplier was processed by means of a frequency analyser (Hewlett/Packard 8553/2) to provide at each point in the flow a velocity probability density distribution. One example of such a distribution is shown in Figure 6 which also gives the equations employed to calculate from the record of the statistical nature of the flow, local flow parameters such as mean velocity, turbulence intensity and higher order correlations of the velocity fluctuations.

3.3 Measurements and Evaluation of the Experimental Data: The measurements were carried out using an experimental method verified by preliminary testing. The water supply system was switched on and a discharge giving a flow Reynolds number of 85,000 obtained by regulating valves at the top and bottom of the test rig. After steady conditions were established, discharge and pressure drop measurements were made for the water flow, followed by a traverse with the laser-Doppler anemometer. The resulting velocity probability density distributions obtained at discrete points in the flow were recorded on an x-y plotter for subsequent evaluation to obtain the required information on the flow. During the laser-Doppler traverse, flow rate and pressure drop measurements were made at frequent intervals to check the steadyness of the flow conditions. It was found that these conditions could be maintained to better than $\pm$ 1%.

For the polymer measurements, carried out at the same Reynolds number, the experimental procedure was similar to that detailed above; the only difference being the incorporation of the polymer supply system. This system was switched on after the water flow had established itself in the channel and the decreased pressure was compensated for by adjusting the downstream valve. After these adjustments the flow system was left for half an hour to reach steady conditions before the final flow rate and pressure drop readings were taken. These were followed by the laser-Doppler measurements as in the case of the water flow.

Evaluation of Velocity Data: The evaluation of the required velocity information from the velocity probability density records was carried out by means of a computer, after manually digitalizing the x-y records of the frequency analyser output. The evaluated data were corrected for errors due to velocity gradients and finite particle transit time. Results of these evaluations are provided in section 4.

Evaluation of the Wall Shear Stress: For the water flow, wall shear stress was evaluated on the basis of a Clauser plot, which is a representation of the well established law-of-the-wall region with the wall shear stress as a parameter. The normalised velocity distribution

$$u^+ = 5.5 \lg y^+ + 5.45$$

may be written as:

$$\frac{u}{u_G} = 5.5 \sqrt{\frac{\tau_w}{\rho u_G^2}} \quad \lg\left(\sqrt{\frac{\tau_w}{\rho u_G^2}} \cdot \frac{y \cdot u_G}{\nu}\right) + 5.45 \sqrt{\frac{\tau_w}{\rho u_G^2}}$$

$$\frac{u}{u_G} = \sqrt{\frac{C_f}{2}} \left[5.5\left(\lg\left(\frac{y \cdot u_G}{\nu}\right) + \lg\sqrt{\frac{C_f}{2}}\right) + 5.45\right]$$

and (u/u_G) then plotted as a function of $\lg(y\,u_G/\nu)$ for different values of C_f. If the experimental results are plotted in this diagram the corresponding C_f value and, hence, the shear stress can be obtained. The value obtained from the Clauser plot compared well with the corresponding value obtained from pressure drop measurements.

$$(u_\tau)_{\text{Clauser}} = 0.0824 \text{ m/s}$$

$$(u_\tau)_{\text{pressure}} = 0.0845 \text{ m/s}$$

In the case of polymer injection an integral value for the shear velocity was obtained from pressure drop measurements. For the wall opposite to the polymer injection system, the wall shear stress was evaluated from a Clauser plot. The following values were obtained

$$(u_\tau)_{\text{integral}} = 0.0704 \text{ m/s} \qquad (u_\tau)_{\text{water}} = 0.0825 \text{ m/s}$$

The shear velocity for the wall opposite to the polymer injection system is seen to be virtually identical to that for the water flow. This indicates that no polymer had diffused to this wall. The significance of this point is commented on in section 4.

Using these data, the shear stress for the polymer flow was calculated to be

$$(u_\tau)_{\text{polymer}} = \sqrt{2(u_\tau)^2_{\text{total}} - (u_\tau)^2_{\text{water}}} = 0.0409 \text{ m/s}$$

4. EXPERIMENTAL RESULTS

The measured overall friction factors for the water and polymer tests are shown in Fig. 4 and indicate an overall drag reduction of 27%. Based on the wall shear stress values calculated in the previous section, the drag reduction is 75%. The difference between the overall reduction and the "local" decrease in wall shear stress is due to the fact that the polymer solution was only injected near one wall.

It is noteworthy that this remarkable reduction was obtained with a 100 ppm polymer solution (Polyox Coagulant) and only 0.14% of the water flow was injected, corresponding to 0.14 g of polymer per cubic meter of water. During the present investigations no attempt was undertaken to maximize drag reduction and still higher values are probable.

Figure 7 shows a Clauser Plot of the mean velocity distribution for water flow and for the wall opposite to the injection system for the polymer flow. Both profiles agree yielding the same wall shear stress and indicate that no polymer had diffused to the opposite wall. This is also indicated in Figure 8 which shows the agreement of the two mean velocity profiles near the wall opposite the injection system.

Figure 8 shows the distributions of mean velocity across the entire test section. The figure shows the shift in the position of maximum velocity in the polymer flow towards the wall where the polymer solution was injected, as would be expected from the lower wall shear stress on this side of the conduit.

Figure 9 shows mean velocity profiles, normalized with data for the maxima of the velocity profiles, that indicate an appreciable difference between the mean velocity profiles for the water and polymer flow. The turbulence intensity distributions show lower values for the polymer flow indicating reduced turbulence production due to the injected polymer.

Figure 10 shows mean velocity data normalized with the shear velocity and plotted versus the normalized distance from the wall. This plot demonstrates that the change in the velocity profile is caused by effects that yield a thickening of the laminar sublayer. In addition, structural changes in the wake region of the flow are indicated resulting from interference of the two wall boundary layers forming at the side walls of the conduit.

The implications of the probability density profiles shown in Figure 11 will be discussed in the following section.

5. DISCUSSION OF THE RESULTS AND FINAL CONCLUSIONS

It has been pointed out in section 1 that one of the objectives of the authors' research programme was to experimentally verify the physical model put forward for the near wall region of turbulent wall boundary layers with and without polymer additives. Section 2 summarizes the major points of the physical model and shows that two different bursting mechanisms exist, refered to as initial and secondary bursting. The present model predicts that the polymer action is to suppress, and in the limit to prevent, the interaction between the near-wall region and the region where the log-law velocity distribution holds and, hence, to suppress and finally prevent sweeping and secondary bursting. Keeping in mind that the interaction of the near wall and the log-law region is intermittent, one can think of the buffer region of a wall boundary layer flow as being made up of contributions from both regions. Hence, if the predictions of the model are correct, one of the results of the polymer action should be the reduction in size of the buffer region. This is indicated by the experimental results shown in Figure 10 . The slightly too high values measured in the sublayer of the polymer flow can presently not be explained and further experiments will be needed to reach final conclusion on the velocity field in the sublayer region.

The suppression of the interaction between the near wall and log-law regions is indicated further by the velocity probability density records in Figure 11a . The sweep time was adjusted by trial and error until the two separated distributions representing the contributions from the near-wall and the log-law regions could be obtained with consecutive sweeps. For the same sweep time , Figure 11b shows for water flows that a separation of the two contributions could not be made due to the higher bursting rate. Figure 11c, obtained from the polymer flow for a slightly longer sweep time shows clearly that the distribution is representative of two processes one of which slightly dominated during the measuring time. The reduced interaction between the near wall and log-law region of turbulent boundary layers with polymer additives is indicated also by the fact that, despite the long distance between the polymer injection system and the measuring cross section, no polymer had diffused to the opposite wall. This is indicated by the Clauser Plot in Figure 7 , which gives the same wall shear stress on the opposite wall with and without polymer injection.

Finally the reader's attention is drawn to the centre part of the conduit flow with polymer injection. Here two boundary layers of different properties interact and large differences in the wake regions of these boundary layers occur, compared with the wake regions of two equal boundary layer flows. This is indicated in Figure 10 and is the subject of further investigations by the authors.

ACKNOWLEDGEMENTS : The authors thank Professor E. Naudascher, leader of the SFB 80, for his assistance throughout this study. The second author thanks the New Zealand Ministry of Works for the study leave during which the work described herein was carried out. Thanks are extended to Mrs.M. Cherdron and Mrs.U. Widdecke for assistance in manuscript preparation.

REFERENCES

(1) Toms, B.A. (1948) : Some Observations on the Flow of Linear Polymer Solutions through Straight Tubes at Large Reynolds Numbers, Proc. 1st. Int. Congress on Rheology, II, p 135, North Holland Publishing Co.

(2) Lumley, J.L. (1969) : Drag Reduction by Additives, Annual Review of Fluid Mechanics, 1, p.367

(3) Lumley, J.L. : Drag Reduction in Turbulent Flow by Polymer Additives, Macromolecular Reviews, in press

(4) Wells, C.S.Jr. and Spangler, J.G. (1967): Injection of a Drag Reducing Fluid into Turbulent Pipe Flow of a Newtonian Fluid , NASA CR-852, LTV Research Center, Dallas, Texas

(5) Kline, S.J., Reynolds, W.C., Schraub, F.A. and Runstadler, P.S. (1967) : The Structure of Turbulent Boundary Layers, Journal of Fluid Mechanics, 30, 4, p. 741

(6) Corino, E.R. and Brodkey, R.S. (1969) : A Visual Investigation of the Wall Region in Turbulent Flow, Journal of Fluid Mechanics, 37, 1, p. 1

(7) Wallace, J.M., Eckelmann, H. and Brodkey, R.S. (1972) : The Wall Region in Turbulent Shear Flow, Journal of Fluid Mechanics, 54, 1, p. 39

(8) Kim, H.T., Kline, S.J. and Reynolds, W.C. (1971) : The Production of Turbulence Near a Smooth Wall in a Turbulent Boundary Layer, Journal of Fluid Mechanics, 50, 1, p. 133

(9) Offen, G.R. and Kline, S.J. (1974) : Combined Dye Streak and Hydrogen Bubble Visual Observations of a Turbulent Boundary Layer, Journal of Fluid Mechanics, 62, 2, p. 223

(10) Donahue , G.L., Tiederman, W.G., and Reischman, M.M. (1972) : Flow Visualization of the Near-Wall Region in a Drag-Reducing Flow, Journal of Fluid Mechanics, 56, 3, p. 559

(11) Wu, J. and Tulin, M.P., (1970) : Drag Reduction by Ejecting Additive Solutions into a Pure Water Boundary Layer, Hydronautics Inc., Technical Report 353-7

(12) Durst, F. and Whitelaw, J.H., (1973) : Light Source and Geometrical Requirements for the Optimization of Optical Anemometry Signals, Opto-Electronics, 5, p. 137

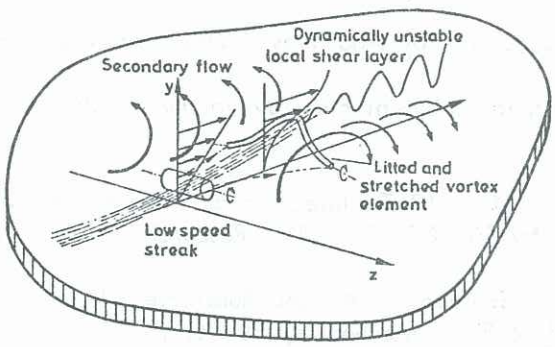

FIG.1: Formation of Initial Burst
(from Kline et. al 1967)

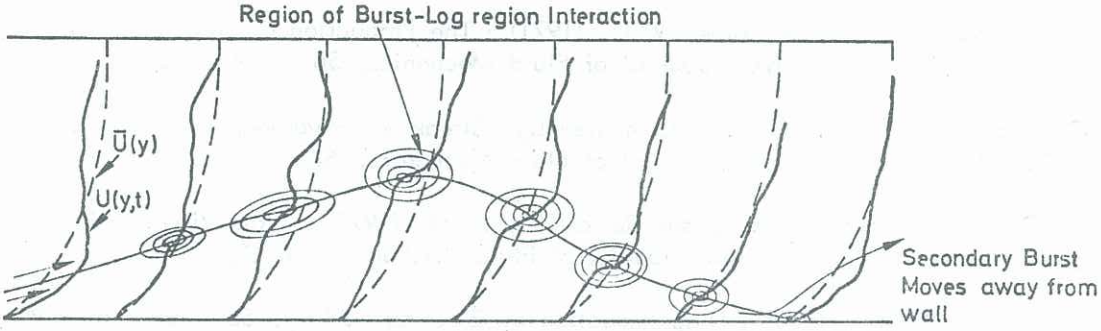

FIG.2: Secondary Burst Formation Cycle (Velocity Profiles from Kim et al 1971)

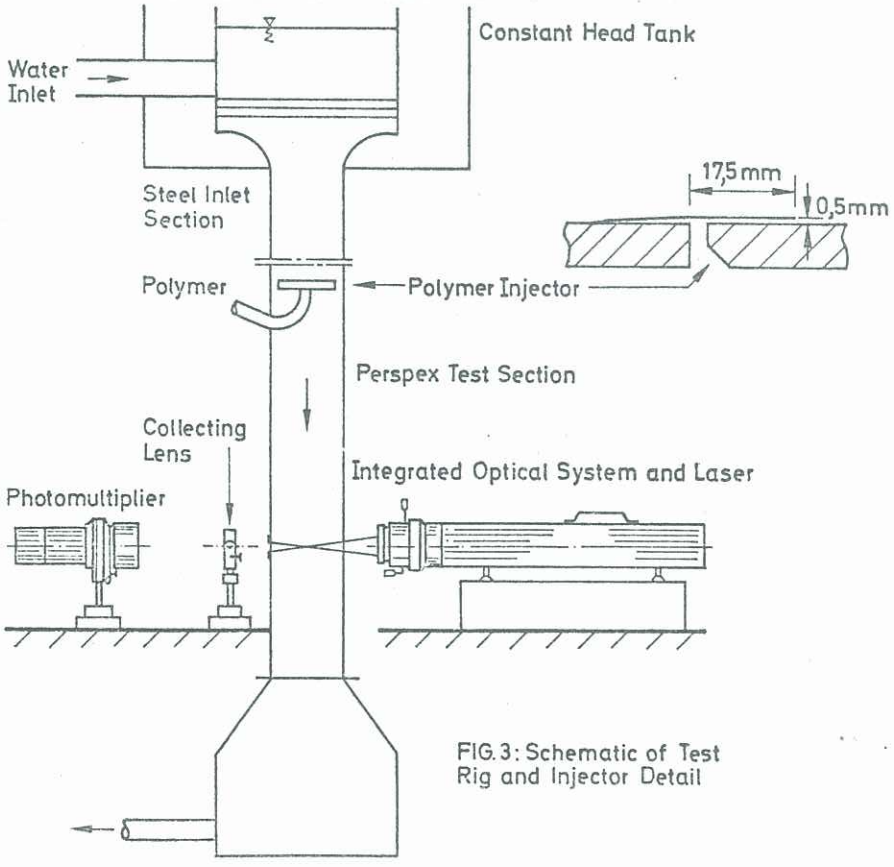

FIG.3: Schematic of Test
Rig and Injector Detail

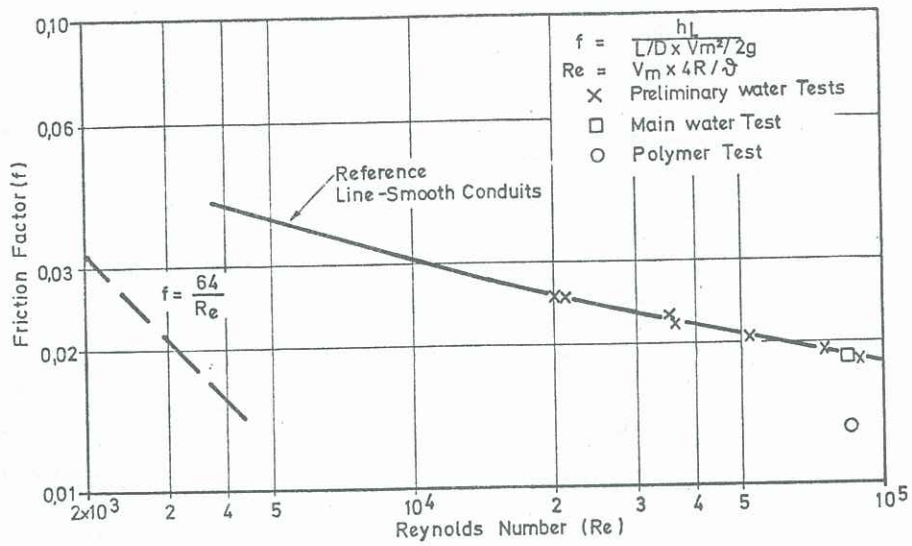

FIG. 4 Friction Factor Data

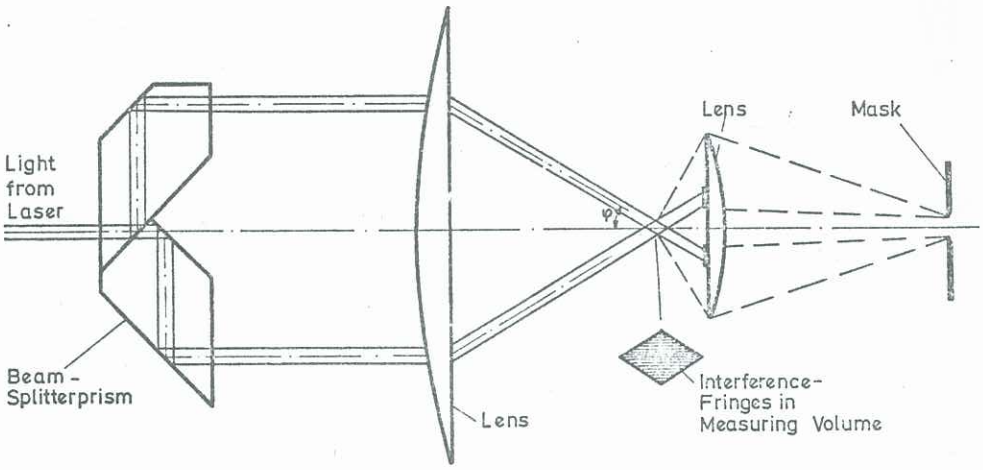

FIG. 5 Schematic of Optical Arrangement Employed for Velocity Measurements

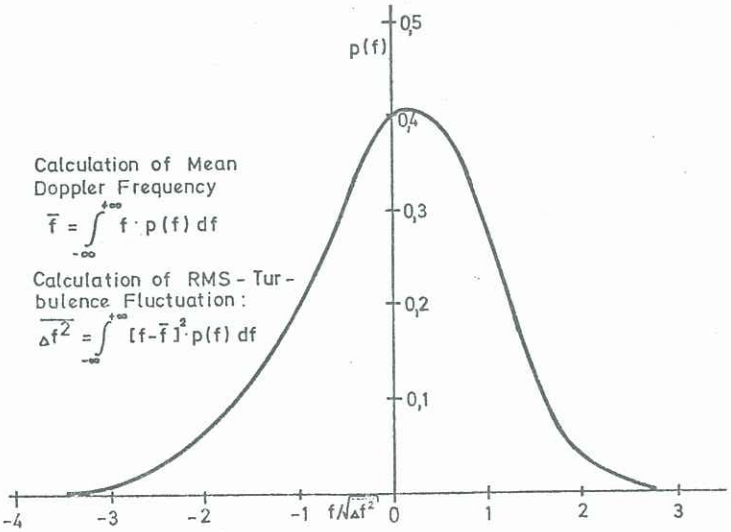

FIG. 6 Frequency probability density Distribution and Calculations of Flow Properties

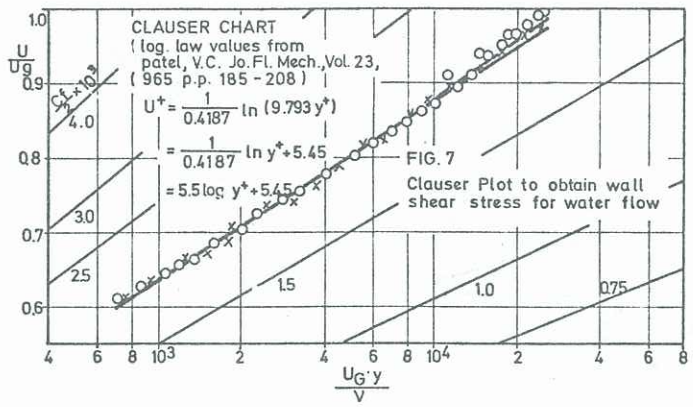

FIG. 7
Clauser Plot to obtain wall shear stress for water flow

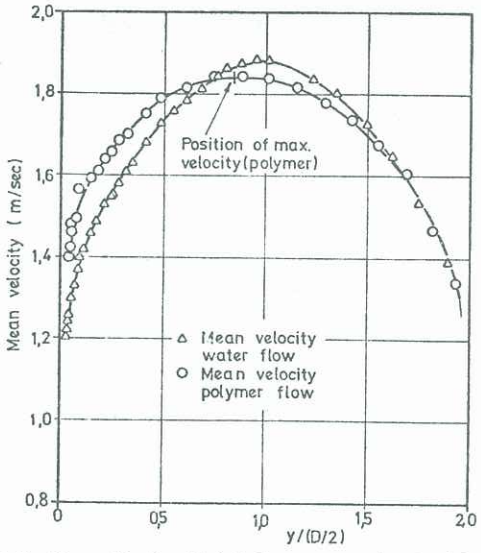

FIG. 8 Mean Velocity Distribution across the Conduit

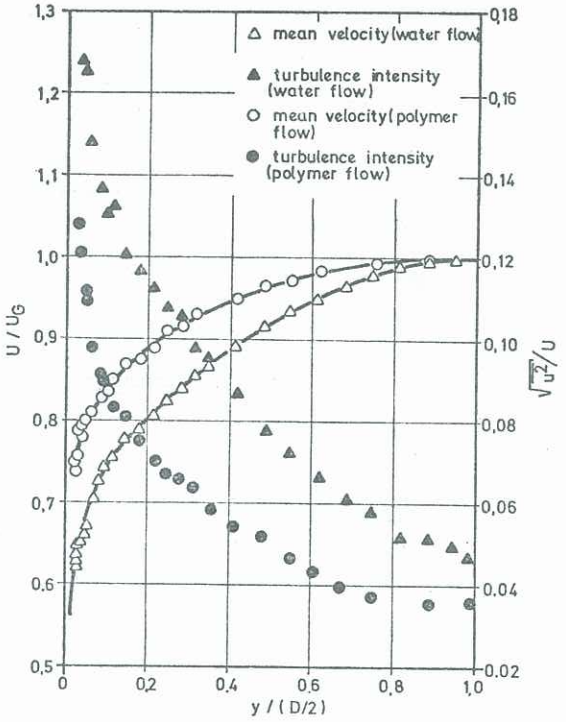

FIG. 9 Normalized Mean Velocity and Turbulence Intensity Distributions for Water and Polymer Flows

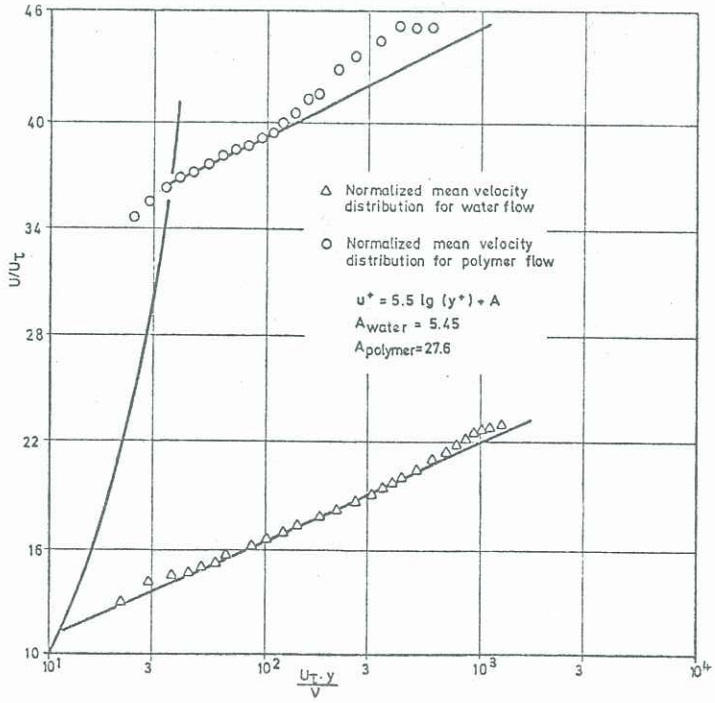

FIG. 10 Normalized Mean Velocity Distribution for Water and Polymer Flows

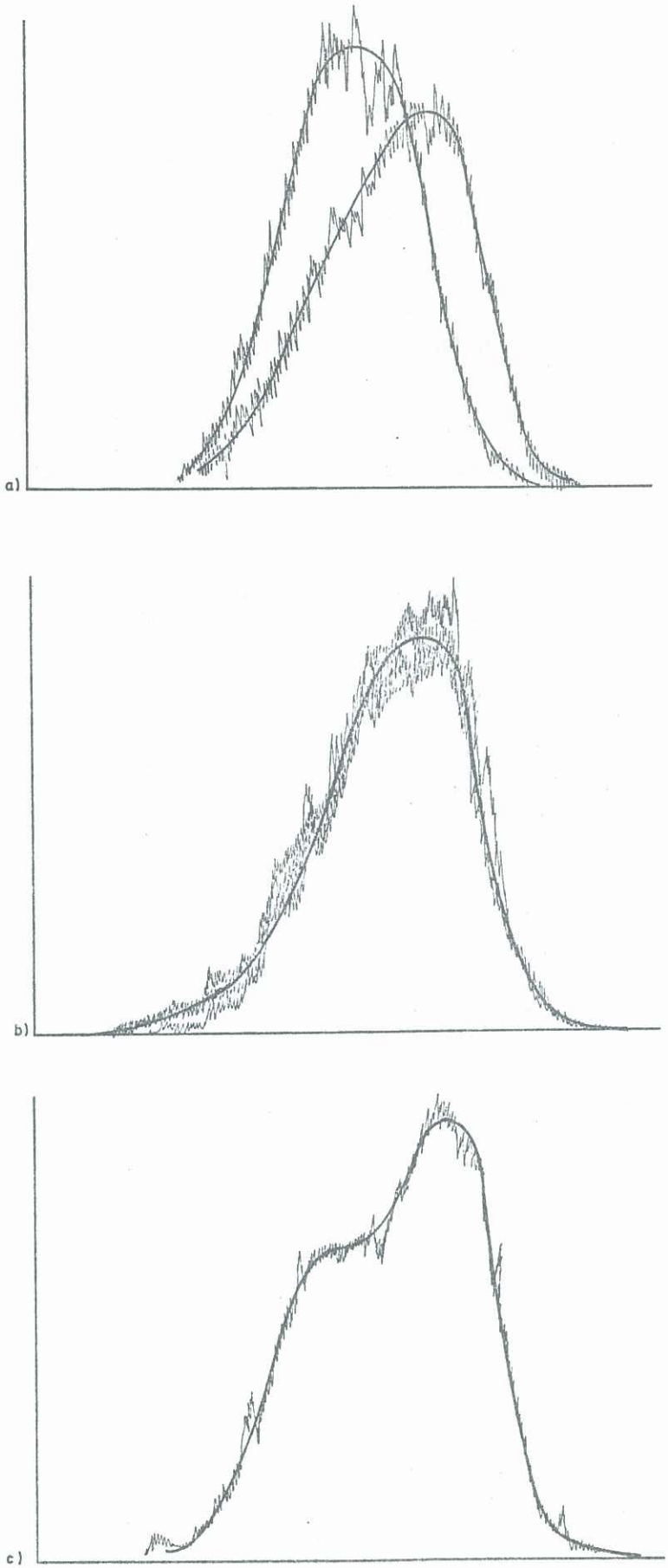

FIG.11 Measured Probability density Distribution